



Harnessing SiC nanoparticle-coated Ni-Al catalysts for more efficient Steam Methane Reforming

Jose Mateo Martinez Saavedra¹, Weberton Reis do Carmo¹, Pedro N. Romano¹, João M.A.R. de Almeida^{1*}

 1 Laboratório de Intensificação de Processos e Catálise (LIPCAT) - UFRJ, Rio de Janeiro, Brasil, j.monnerat(@iq.ufrj.br

Resumo/Abstract

ABSTRACT – The development of stable and efficient catalysts for Steam Methane Reforming (SMR) remains a critical challenge due to catalyst deactivation caused by coke deposition and metal sintering. In this study, Ni-Al coated SiC nanoparticle catalysts (Ni-Al@SiC) were synthesized using a hydrotalcite precursor route, aiming to enhance thermal stability and catalytic performance. Structural and chemical characterization, including XRD, SEM-EDS, N2 physisorption, and MAS NMR analyses, confirmed the successful embedding of SiC within the Ni-Al matrix. Catalytic evaluation demonstrated that Ni-Al@SiC catalysts exhibited superior Unlike conventional approaches, the incorporation of SiC nanoparticles (100 nm) within the catalyst matrix led to improved heat management and metal dispersion stability, showing no deactivation after 70 hours on stream. Furthermore, the Turnover Frequency (TOF) analysis indicated enhanced catalytic efficiency with reduced active phase requirements, attributed to SiC's superior thermal conductivity and uniform heat distribution. Notably, the presence of SiC mitigated local hot spots, counteracting the endothermic nature of the SMR reaction. These findings highlight the potential of Ni-Al@SiC catalysts to improve SMR efficiency, offering promising avenues for future research and industrial application.

Keywords: Steam Methane Reforming (SMR), SiC nanoparticles, Catalyst stability

Introduction

Hydrogen is a fundamental raw material for numerous industrial processes and a key fuel for decarbonization due to its high combustion power and CO₂-free combustion. However, despite its sustainable potential, hydrogen production still has a high CO2 footprint, and storage remains challenging [1]. Currently, most hydrogen is produced via Steam Methane Reforming (SMR), which operates at high temperatures (650-900 °C) and requires significant steam input (H₂O:CH₄ molar ratio of 3:1), resulting in considerable CO₂ emissions—approximately 12 kg of CO₂ per kg of H₂ produced [2]. This footprint can be reduced to 4 kg CO₂/kg H₂ with 90% CO₂ capture using Carbon Capture and Storage (CCS) technologies [3]. Additionally, process efficiency improvements through catalysts with higher activity and stability can further reduce emissions.

One of the main challenges in SMR is minimizing catalyst deactivation caused by coke formation and metal sintering, which are exacerbated by the highly endothermic nature of the reaction[4]. Cold spots can form during the reaction, promoting coke deposition, while increasing the temperature to mitigate this risk may lead to metal phase sintering, reducing catalytic activity. Catalyst support plays a critical role in enhancing stability by promoting optimal metal dispersion, minimizing sintering, and improving reagent mixing to reduce secondary reactions[5].

Coke formation and metal sintering can be mitigated using two strategies: (1) employing basic supports (e.g., CaO, MgO, CeO₂, La₂O₃) that suppress carbonaceous precursor adsorption and promote water dissociation into

reactive hydroxyl groups for carbon gasification [6], or (2) using thermally conductive supports to prevent temperature gradients[7]. Among such materials, SiC is particularly promising due to its excellent thermal conductivity, high heat capacity, low thermal expansion coefficient, and robust mechanical and chemical stability, making it highly suitable for heterogeneous catalysis applications[8].

The incorporation of silicon carbide (SiC) into Ni-based catalysts for Steam Methane Reforming can enhance thermal stability and catalytic performance due to SiC's excellent thermal conductivity and mechanical stability. However, its effectiveness depends on the synthesis method and metal-support interactions.

Lee et al. [9] developed Ni/SiC@Al₂O₃ core-shell catalysts via a hydrothermal method, achieving improved heat transfer and mechanical stability. Despite these advantages, deactivation occurred due to coke formation and Ni sintering, attributed to large Ni particle size and limited Al₂O₃ content. Shen et al. [10] prepared monolithic Ni-SiC catalysts using freeze-gelation, yielding high thermal conductivity and reduced hotspots, which enhanced methane conversion (up to 86% at 800 °C). In contrast, Garcia-Vargas et al. [11] found that Ni-Mg/SiC catalysts' performance varied with the metal impregnation order, with initial Ni impregnation resulting in poor activity due to weak Ni-Mg interactions and Ni₂Si formation.

Overall, these studies highlight that incorporating SiC into SMR catalysts can improve thermal management and stability, but optimizing synthesis methods and metal-support interactions is essential. In this work, Ni-Al-coated SiC catalysts (Ni-Al@SiC) were synthesized using SiC



nanoparticles as a novel strategy to minimize Ni sintering through weaker Ni-SiC interactions and enhance heat dispersion.

Experimental

Catalysts preparation.

Ni–Al@SiC catalysts were synthesized via a hydrotalcite precursor route using a hydrothermal method, incorporating SiC nanoparticles within the catalyst matrix to enhance thermal properties and structural stability according to H. Lee et al. [9]. Three catalysts were prepared with SiC (100 nm) loadings of 0, 25, and 50 wt%, maintaining a nominal Ni:Al molar ratio of 3:1. The initial SiC mass was kept constant, resulting in lower Ni and Al concentrations in the final materials with increasing SiC content, a factor that warrants discussion. Table 1 presents the theoretical Ni and Al contents for each formulation. The hydrotalcite synthesis yield, defined as the percentage of initial Ni and Al incorporated into the final product, was approximately 25% for all samples.

Table 1. Theoretical mass composition of the Ni-Al@SiC based-

catalysts.

Ni-Al@SiC	Ni-Al@SiC	Ni-Al@SiC	C	
vt. %)	(50 wt.	(25 wt. %)	(0 wt. %)	Compound
13	43	65	87	Ni
7	7	10	13	Al
50	50	25	0	SiC
4		25	0	SiC

The synthesis began by dispersing 2.0 g of SiC powder and 5.33 g of polyethylene glycol in 25 mL of deionized water under ultrasonic treatment and vigorous stirring. Separately, a solution was prepared by dissolving 6.98 g of Ni(NO₃)₂·6H₂O, 3 g of Al(NO₃)₃·9H₂O, and 4.84 g of urea in 10 mL of deionized water. This precursor solution was subsequently combined with the SiC dispersion. The initial pH of the mixture was adjusted to 2 by adding a few drops of diluted nitric acid (1 M). The hydrothermal synthesis was performed in a Teflon-lined autoclave (100 mL capacity) at 90 °C for 24 hours.

After the reaction, the resulting material was centrifuged, thoroughly washed with deionized water, filtered, and dried at 80 °C for 12 hours. A portion of the dried material was then calcined at 750 °C for 4 hours to obtain the final catalyst. The hydrotalcite-derived catalysts were labeled as Ni-Al-LDH@SiC, while the calcined materials were designated as Ni-Al@SiC.



Characterization.

The textural and morphological properties of the catalysts were characterized using XRD, SEM-EDS, and N₂ physisorption. Additionally, the chemical nature of Si and Al in the supports was investigated through MAS-NMR of ²⁹Si and ²⁷Al. Post-reaction catalysts were analyzed by SEM and TGA to assess Ni sintering and coke deposition.

Steam Methane Reforming reaction test.

The catalytic activity was evaluated for the Steam Methane Reforming (SRM) reaction at 650 °C and 2 bar pressure, using the following volumetric standard flows: 25 mL/min of CH₄, 25 mL/min of N₂, and 0.056 mL/min of liquid water, maintaining a molar H₂O:CH₄ ratio of 3:1. Before entering the reactor, water was vaporized, and all gases were preheated to 200 °C.

Each test utilized 0.1 g of catalyst, which was activated prior to the reaction by heating at a controlled rate of 5 °C/min to a temperature of 700 °C under a 25 mL/min hydrogen flow and holding this condition for 30 minutes to ensure proper catalyst activation.

Results and Discussion

The formation of the hydrotalcite phase and its subsequent transformation upon calcination were confirmed by XRD analysis. Figure 1 displays the diffraction patterns of the as-synthesized samples, where characteristic reflections of hydrotalcite are observed, Figure 1A. As expected, no SiC-related peaks were detected in the SiC-free sample. In contrast, distinct SiC diffraction signals were identified in the samples containing 25 wt.% and 50 wt.% SiC, with notably higher peak intensity in the latter, consistent with increased SiC content.

Upon calcination, Figure 1B, the disappearance of hydrotalcite reflections and the emergence of NiO peaks dominate the diffractograms, attributed to the high Ni loading relative to Al across all formulations, and confirming the formation of NiO.

Table 2 presents the surface area values of both the precursor materials and the final catalysts. As shown, the precursors—layered double hydroxides (LDHs)—exhibit lower surface areas compared to their corresponding calcined forms, a typical characteristic of this class of materials. The LDHs possess compact, tightly stacked layers stabilized by electrostatic interactions and hydrogen bonding with interlayer water molecules, which limits their porosity and results in relatively low surface areas.



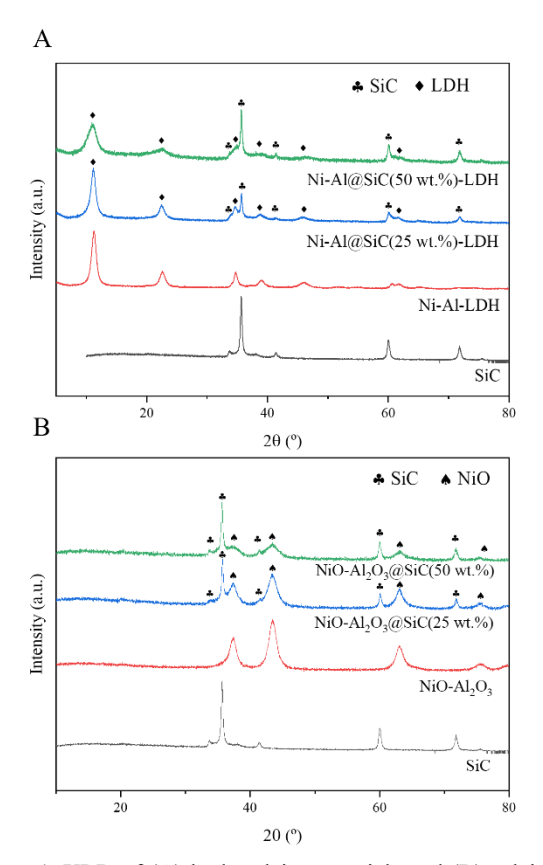


Figure 1. XRD of (A) hydrotalcite materials and (B) calcined materials.

 Table 2. Surface area of precursors and final catalysts.

Precursor	Ni-Al- LDH@SiC (0 wt. %)	Ni-Al- LDH@SiC (25 wt. %)	Ni-Al- LDH@SiC (50 wt. %)
Surface area (m ² /g)	43	48	47
Catalysts	Ni-Al@SiC	Ni-Al@SiC	Ni-Al@SiC
	(0 wt. %)	(25 wt. %)	(50 wt. %)
Surface area (m ² /g)	140	102	99

After calcination, the collapse of the layered structure leads to the formation of mixed metal oxides with increased porosity and surface area. Additionally, Table 2 shows that the SiC-free catalysts have higher surface areas than their SiC-containing counterparts. This reduction is attributed to the intrinsically poor textural properties of silicon carbide, which may dilute or the overall porosity of the catalyst matrix.

Figure 2 shows the ²⁹Si and ²⁷Al MAS NMR spectra of Ni–Al@SiC catalysts with varying SiC contents (0 wt.%, 25 wt.%, and 50 wt.%). The ²⁷Al spectrum for the SiC free and 25 wt.% SiC catalysts exhibits broad and noisy signals,



likely due to high Ni content interfering with the measurement.

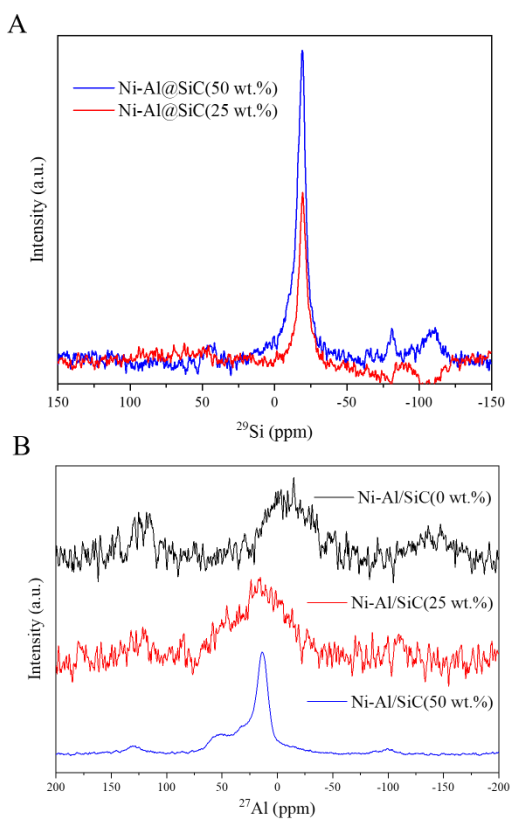


Figure 2. 29 Si and 27 Al MAS NMR Spectra of Ni-Al@SiC Catalysts.

In contrast, the 50 wt.% SiC catalyst displays more defined peaks at approximately 12-13 and 53-55 ppm, attributed to lower Ni content. The signal observed at 12–13 ppm in the ²⁷Al MAS NMR spectrum is attributed to octahedrally coordinated aluminum species (AlO₆), which are commonly associated with aluminum hydroxides or partially hydrated environments [12]. In contrast, for pure γalumina, the octahedral aluminum resonance typically appears around 4-6 ppm. The shift of the octahedral signal to higher chemical shifts in our sample can be explained by the altered local electronic environment surrounding the aluminum atoms. Specifically, the presence of neighboring atoms such as nickel, silicon, and carbon-introduced during synthesis may perturb the aluminum framework through electronic interactions or structural distortions. The higher electronegativity and electronic affinity of these heteroatoms can influence the electron density around the aluminum nuclei, leading to a de-shielding effect and, consequently, a downfield shift in the NMR signal. This phenomenon is consistent with previous reports on aluminum-containing materials modified with transition metals or heteroatoms, where local coordination and



electronic effects cause noticeable variations in chemical shift [12]. The peak at 55 ppm corresponds to tetrahedrally coordinated aluminum (AlO₄), which falls within the chemical shift range commonly reported in the literature [12]. Regarding the ²⁹Si analysis, catalysts with 25 and 50 wt.% SiC (Figure 2-A) show a sharp intense peak, characteristic of crystalline SiC.

SEM-EDS images, Figure 3, shows the presence of thin lamellar structures across all formulations, which appear to coat the SiC particles—except in the SiC-free sample. In the absence of SiC, the lamellae exhibit a rosette-like morphology, forming large, aggregated structures. Also, the SEM-EDS mapping of all samples, confirming the homogeneous distribution of Ni, Al, and Si throughout the entire structure in all three formulations. After calcination, the lamellar structures were preserved, as well as the element distribution.

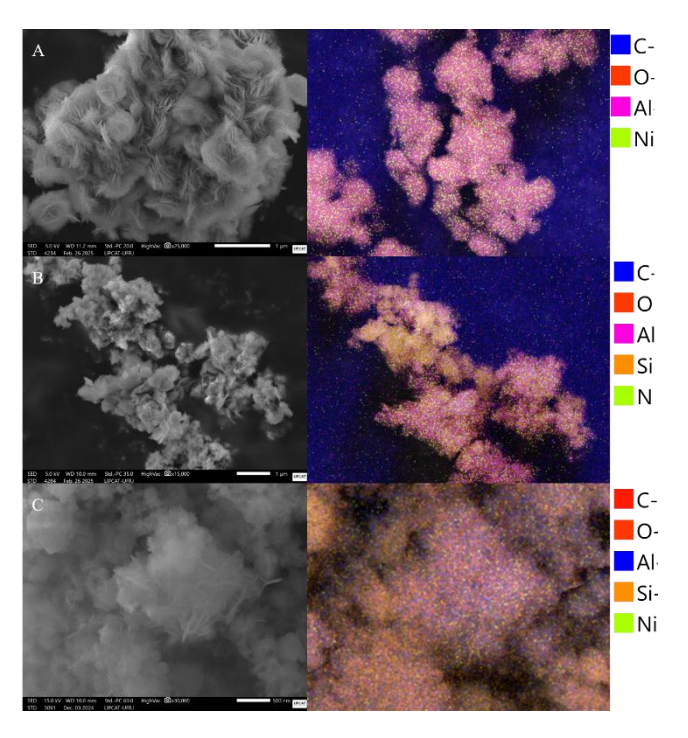


Figure 3. SEM-EDS pictures of the hydrotalcite materials before calcination. (A) Ni-Al-HDT, (B) Ni-Al@SiC(25 wt.%)-HDT, (C) Ni-Al@SiC(50 wt.%)-HDT.

STEM-EDS images of the catalyst containing 50 wt% SiC, revealing that the SiC nanoparticles are fully embedded and coated by Ni and Al oxides, Figure 4. The integration of SiC within the oxide matrix indicates effective dispersion and incorporation of the nanoparticles into the catalyst interior.



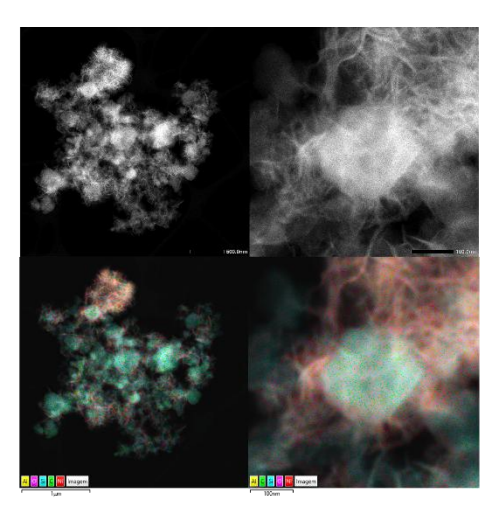


Figure 4. STEM-EDS Mapping of Ni-Al Coated SiC Nanoparticles.

Figure 5 presents the main results of the catalytic test for steam methane reforming (SMR) conducted with the materials used in this study. Figure 5-A shows the catalytic activity given as methane conversion as a function of time on stream, while Figure 5-B expressed the methane conversion rates normalized to total Ni contents (mol_{CH4}/s.g_{Ni}). The normalized conversion was calculated using the theoretical Ni calculated from the mass balance of the synthesis. Both curves show that the three catalysts need a stabilization time of 11 h, probably because the reduction of these catalysts were performed in conditions of the supported catalysts which have a lesser amount of Ni. The catalyst without SiC exhibited deactivation over time, whereas the SiC-containing catalysts showed no deactivation; instead, they displayed a slight increase in activity over time.

Since SiC is incorporated into the bulk of the catalyst, its concentration directly influences the Ni content, thereby altering the number of active sites available for the reaction. In principle, an increased number of active sites should enhance catalytic activity. On account for these variations, the catalytic performance was evaluated in terms of methane conversion rate normalized by the theoretical Ni in the catalysts. The results indicate that catalysts with higher SiC content exhibit superior normalized conversion values. This enhancement can be attributed to multiple factors. First, increasing the SiC fraction reduces the overall Ni content in the catalyst, which may lead to differences in Ni dispersion and particle size. A lower Ni loading could promote better dispersion, increase the fraction of exposed active sites and improve intrinsic catalytic activity.

Additionally, SiC's high thermal conductivity may contribute to more efficient heat distribution within the catalyst. This effect is particularly relevant for endothermic reactions, such as steam methane reforming (SMR), where localized overheating or cold spots can impact reaction rates



and carbon deposition. By facilitating uniform heat transfer, SiC could mitigate thermal gradients, enhancing reaction efficiency and catalyst stability over time. Thus, the observed improvements in normalized conversion for SiC-containing catalysts suggest a relationship effect between Ni dispersion and thermal management, highlighting the potential of SiC nanoparticles as a structural and thermal promoter in catalytic systems.

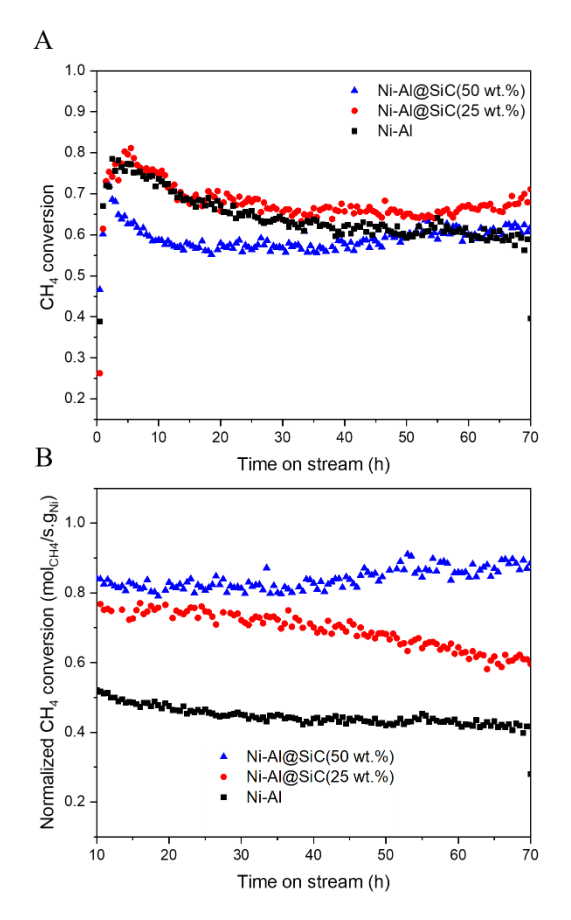


Figure 5. Steam Methane Reforming Performance of Hydrotalcite-Derived Catalysts Coated with SiC.

SEM image of the spent catalyst containing 50 wt.% SiC, revealing a significant presence of nanotubular coke on the catalyst surface, Figure 6. Despite the substantial coke formation, catalytic activity remained largely unaffected, as the coke did not fully cover the Ni clusters, which are still visible in the image.

This observation is consistent with the DTG analysis presented in Figure 7, which indicates that approximately 40% of the spent catalyst consists of coke after 70 hours of reaction. Notably, all the coke formed decomposes at temperatures above 600 °C, confirming the presence of fibrous coke that does not significantly impair catalytic performance.



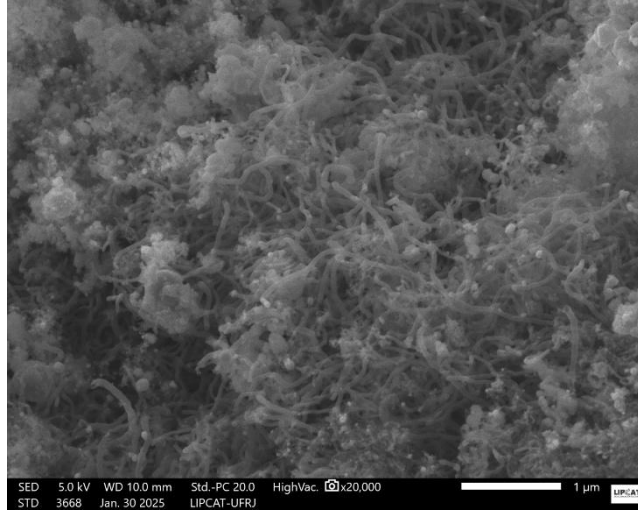


Figure 6. SEM picture of spent Ni-Al@SiC(50 wt.%) catalysts.

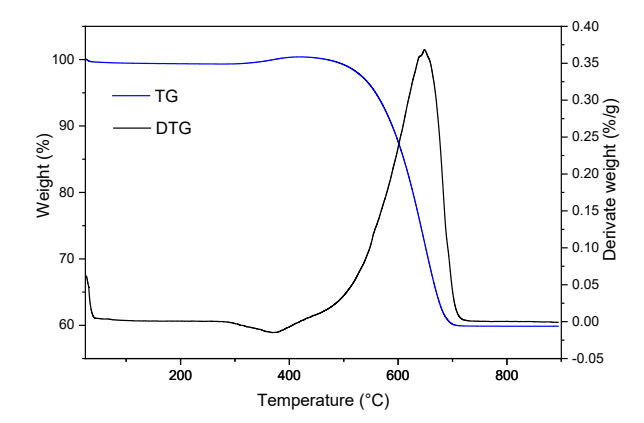


Figure 7. TG and DTG of spent spent Ni-Al@SiC(50 wt.%) catalysts

Conclusions

Ni-Al coated SiC nanoparticle catalysts (Ni-Al@SiC) were successfully synthesized using a novel approach aimed at incorporating smaller SiC nanoparticles to develop more stable and efficient catalysts for Steam Methane Reforming (SMR). The detailed characterization revealed that the SiC nanoparticles were effectively embedded within the Ni-Al matrix, forming a well-dispersed structure.

SMR performance tests demonstrated that catalysts containing SiC exhibited significantly enhanced stability, showing no deactivation after 70 hours on stream. Furthermore, normalized methane conversion analysis indicated that the inclusion of SiC led to more efficient catalysts, requiring a lower active phase content to maintain similar catalytic performance compared to SiC-free counterparts. This improvement is primarily attributed to the superior thermal conductivity of SiC, which promotes uniform heat distribution and mitigates the cold spots



typically caused by the endothermic nature of the SMR reaction.

Moreover, the SEM analysis of spent catalysts confirmed that despite the formation of nanotubular coke, the catalytic activity remained unaffected due to the coke's fibrous nature, which did not obstruct the active Ni sites. The combination of enhanced thermal stability and efficient heat management makes these Ni-Al@SiC catalysts promising candidates for more efficient SMR processes. This novel approach offers a valuable pathway for the development of advanced catalytic systems for hydrogen production.

Acknowledgments

We acknowledge Qatar Energy and UFRJ University for funding support.

References

- [1] "F.S. AlHumaidan, M. Absi Halabi, M.S. Rana, M. Vinoba, Blue hydrogen: Current status and future technologies, Energy Conversion and Management 283 (2023) 116840. https://doi.org/10.1016/j.enconman.2023.116840. - Buscar con Google". Acesso em: 16 de maio de 2025.
- [2] "Technological evolution of large-scale blue hydrogen production toward the U.S. Hydrogen Energy Earthshot | Nature Communications". Acesso em: 16 de maio de 2025. Disponível em: https://www.nature.com/articles/s41467-024-50090-w
- [3] "Blue Hydrogen Industry Research 2024: Increased R&D".
- [4] J. O. Ighalo e P. B. Amama, "Recent advances in the catalysis of steam reforming of methane (SRM)", *Int. J. Hydrog. Energy*, vol. 51, p. 688–700, jan. 2024, doi: 10.1016/j.ijhydene.2023.10.177.
- [5] S. Katheria, A. Gupta, G. Deo, e D. Kunzru, "Effect of calcination temperature on stability and activity of Ni/MgAl₂O₄ catalyst for steam reforming of methane at high pressure condition", *Int. J. Hydrog. Energy*, vol. 41, n° 32, p. 14123–14132, ago. 2016, doi: 10.1016/j.ijhydene.2016.05.109.
- [6] "Fabrication of a regenerable Ni supported NiO-MgO catalyst for methane steam reforming by exsolution Korea Advanced Institute of Science and Technology".
- [7] C. Fukuhara, K. Yamamoto, Y. Makiyama, W. Kawasaki, e R. Watanabe, "A metal-honeycombtype structured catalyst for steam reforming of methane: Effect of preparation condition change on reforming performance", *Appl. Catal. Gen.*, vol. 492, p. 190–200, fev. 2015, doi: 10.1016/j.apcata.2014.11.040.



- [8] W. Chen *et al.*, "Intensified microwave-assisted heterogeneous catalytic reactors for sustainable chemical manufacturing", *Chem. Eng. J.*, vol. 420, p. 130476, set. 2021, doi: 10.1016/j.cej.2021.130476.
- [9] "Synthesis Chemistry and Properties of Ni Catalysts Fabricated on SiC@Al2O3 Core-Shell Microstructure for Methane Steam Reforming". Acesso em: 16 de maio de 2025. [Online]. Disponível em: https://www.mdpi.com/2073-4344/10/4/391
- [10] Z. Shen, S. A. Nabavi, e P. T. Clough, "Design and performance testing of a monolithic nickel-based SiC catalyst for steam methane reforming", *Appl. Catal. Gen.*, vol. 670, p. 119529, jan. 2024, doi: 10.1016/j.apcata.2023.119529.
- [11] J. M. García-Vargas, J. L. Valverde, J. Díez, P. Sánchez, e F. Dorado, "Preparation of Ni–Mg/β-SiC catalysts for the methane tri-reforming: Effect of the order of metal impregnation", *Appl. Catal. B Environ.*, vol. 164, p. 316–323, mar. 2015, doi: 10.1016/j.apcatb.2014.09.044.
- [12] L.H. Chagas, G.S.G. De Carvalho, R.A.S. San Gil, S.S.X. Chiaro, A.A. Leitão, R. Diniz, "Obtaining aluminas from the thermal decomposition of their different precursor: An 27Al MAS NMR and X-ray powder diffraction studies", *Materials Research Bulletin.*, Vol 49, p. 216-222, jun. 2014, doi.org/10.1016/j.materresbull.2013.08.072.